

## Demonstration of Readiness for the RTO Transition of the Assimilation of High-Resolution Satellite Soundings into NOAA Operational Regional NWP Models

William L. Smith Sr. (UW/SSEC), Qi. Zhang (HU), and M. Goldberg (NOAA)

**Introduction:** This paper shows the Research To Operations (RTO) transition readiness for the assimilation of hyperspectral infrared satellite sounding radiances into NOAA regional operational NWP models. Because improvements in regional convective weather forecasts have been demonstrated continuously, on a real-time routine basis, during the past two years, it is proposed to begin this RTO demonstration of operational readiness.

Satellite polar satellite hyperspectral radiances are now assimilated into operational Numerical Weather Prediction (NWP) models (Geer et. al., 2018, LeMarshall et. al., 2007, Lin et al., 2017). However, the use of polar satellite hyperspectral radiances for regional short range forecasting has been limited by the relatively poor spatial resolution of the measurements, the latency of the data for the timely assimilation required, and the influence of cloud and surface radiance emission on the measurements which limit their used for the troposphere and over land. Recently, a joint University of Wisconsin and Hampton University project has provided a low latency high-resolution thermodynamic sounding retrieval system made possible through the support of the NOAA JPSS Proving Ground and Risk Reduction and the NASA MUREP Center for Atmospheric Research and Education (CARE) programs. These temperature and moisture soundings are produced at a 2-km spatial and 20 - 30 minute temporal resolution from Direct Broadcast System (DBS) operational polar satellite hyperspectral (i.e., CrIS and IASI) and geostationary satellite multispectral (i.e., ABI) radiances observed over much of the continental US (CONUS) and the Western Atlantic (i.e., 10 – 48 N, 60 to 105 W). High resolution (2-km hourly interval) combined polar hyperspectral (i.e., CrIS and IASI) and Geo-multispectral (GOES-ABI) Temperature and humidity profiles (called “PHSnABI”) are continuously assimilated hourly into 8-km and 3-km spatial resolution Rapid Refresh (RAP) and High Resolution RAP (HRRR) like WRF models (Benjamin et. al., 2016) to investigate the ability of these data for improving the skill of short-term (1 – 12 hour) convective weather forecasts and longer-term (3 – 73 hour) tropical storm and hurricane forecasts. The satellite soundings simulate the high spatial and temporal resolution soundings that could be provide by a geostationary satellite hyperspectral sounding instrument.

The manner in which the atmospheric profile retrievals are assimilated using the model background profiles to de-alias the vertical structure of the retrievals (Smith at. al., 2015, Smith and Weisz, 2017) makes their assimilation equivalent to radiance assimilation, assuming that all the spectral channel radiances with the same spectral resolution and the same instrument and forward model noise levels are used for the radiance assimilation process as used to produce the retrievals (Magliorini, 2011). The practical difference between radiance and retrieval assimilation relates to the computational efficiency and the ability to handle all the physical variables (e.g., clouds, surface skin temperature and emissivity, trace gases, etc.,) that must be accounted for when relating the spectral radiances to the forecast model atmospheric temperature and moisture profile variables. Since hyperspectral sounding instruments contain thousands of spectral channels of information, it is computationally challenging to be able to assimilate all the spectral radiance observations at all the measurement locations. Since the number of model levels is more than an order of magnitude smaller than the number of spectral radiance channels,

assimilating all the spectral information content through profile retrieval greatly increases the computational efficiency of the assimilation process and enables the use of the observations at all measurement locations. In performing atmospheric profile retrievals, all the physical variables that affect the interpretation of the radiances in terms of the atmospheric temperature and moisture profiles, can be determined using the complete spectrum of measurements, which contain all the information needed. This increased computational efficiency and information content, enabled by profile retrieval assimilation, is particularly important for assimilating PHSnABI soundings, which have a horizontal spacing of 2-km and need to be assimilated with high accuracy and low latency on an hourly basis for short-term convective scale weather forecasting.

The joint UW/HU satellite sounding and numerical weather forecast system has been operational for the past two years with the results demonstrating significant improvements in precipitation forecasts associated with both tropical and extra-tropical storms (Shao and Smith, 2019 and Smith et. al, 2020) as well as providing improvements in STP (i.e., Significant Tornado Parameter) forecasts, as is important for warning the public to prepare for the onset of severe convective weather (e.g., high winds, intense precipitation and flash floods, hail, and tornadoes). Also, in support of the development of a US geo-hyperspectral sounding capability, an Observational System Experiment (OSE) forecast impact study, supported by UW-SSEC internal research funds, has been conducted using CrIS and IASI sounding observations obtained prior to the devastating tornado outbreak that occurred near Moore Oklahoma on May 20, 2013. This short note is provided to reveal recent findings revealed through the conduct of the routine DBS satellite sounding and weather forecast operation and the May 20, 2013 tornado outbreak OSE.

### **Winds Derived from Continuous Assimilation of Temperature and Water Vapor**

**Soundings:** It is shown that Wind vectors can be accurately diagnosed through high frequency (i.e., hourly) assimilation of the high-resolution satellite temperature and moisture sounding data over a three-hour spin-up period used to initialize a numerical forecast model. The continuous assimilation of these thermodynamic data enables the model dynamics (i.e., winds) to adjust to the actual motion of the atmosphere through the time integration of the model's equations of motion.

The 3-hour assimilation process used here is illustrated in figure 1. The process begins by using NOAA's Rapid Refresh (RAP) model analysis, which contains all the operationally available meteorological data to which PHSnABI retrievals are assimilated using the Grid-point Statistical Interpolation (GSI) system (James and Benjamin, 2017). From this PHSnABI data modified forecast background, a 1-hour WRF model forecast of the atmospheric state parameters is produced to which the next hour of PHSnABI soundings are assimilated. A second 1-hour WRF forecast is produced and used to assimilate the next hour of PHSnABI soundings. Finally a third 1-hr WRF forecast is produced to which the third hour of PHSnABI data are assimilated. The third hourly forecast provides model diagnosed wind vectors, derived from the three hours of satellite thermodynamic soundings, which are used with the satellite soundings to provide an initial analysis for an hourly interval updated WRF model 12-hour forecast cycle. In principle, the PHSnABI soundings enhance the RAP/HRRR analysis of conventional surface and upper air data, used to begin the 3-hour spin up period for each forecast cycle, that provide improved forecasts.

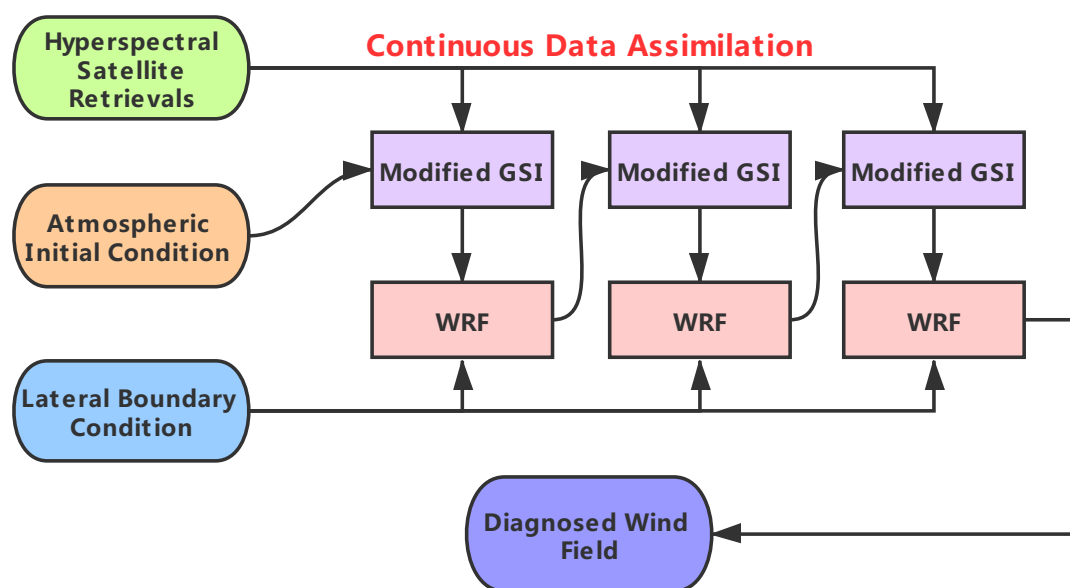


**Figure 1:** A schematic illustrating the 3-hour PHSnABI sounding data assimilation cycle used to diagnose the atmosphere’s wind field, which are used in addition to the latest available PHSnABI temperature and moisture soundings to initialize a 0 to 12 hours weather forecast.

A comparison between the 3-hour spin-up period assimilated PHSnABI model-diagnosed winds at 00 UTC and 12 UTC were compared with CONUS rawinsonde observations and cloud and water vapor track winds obtained throughout the entire month of June 2020. The comparisons were made with the 00 UTC and 12 UTC radiosondes which have not yet been assimilated into the RAP model forecast system used for the de-aliasing of the PHSnABI retrievals used during the spin-up period used to provide the initial conditions for the 12-hour forecast cycle. Figure 2 shows statistics for the differences between model-diagnosed wind vectors and CONUS rawinsonde observations together with statistics for differences between cloud and water vapor feature tracked motion vectors and rawinsonde observations. The cyan curves refer to the 3-hour spin-up cycle model diagnosed winds for the control (i.e., CTL) conducted without the assimilation of PHSnABI soundings, the red curves denote the rawinsonde comparisons with the PHSnABI data assimilation over the 3-hr spin-up WRF forecast model spin-up period (i.e., Model DA3hrs), and the green curve shows the difference between the cloud and water vapor feature tracked wind estimates and the rawinsonde observations, as well as the model diagnosed wind vector differences with the rawinsonde observations for exactly the same locations and times of the feature tracked winds estimates. As can be seen the model diagnosed retrieval assimilated winds are in better agreement with the rawinsonde observations, particularly in the lower troposphere (i.e., below the 500-hPa level) than is the control (i.e., satellite soundings excluded) and the feature tracked winds. Moreover, it is important to note that the model-diagnosed winds are provided for every model vertical level and spatial grid point location, regardless of cloudiness. Because of the four dimensionality of the forecast model, the assimilation of the satellite soundings impacts the model dynamics (i.e., winds), regardless of cloudiness, and satellite observation time and location. Thus, hourly assimilation of high-resolution temperature and humidity soundings improve the model background conditions so as to improve numerical weather forecasts.

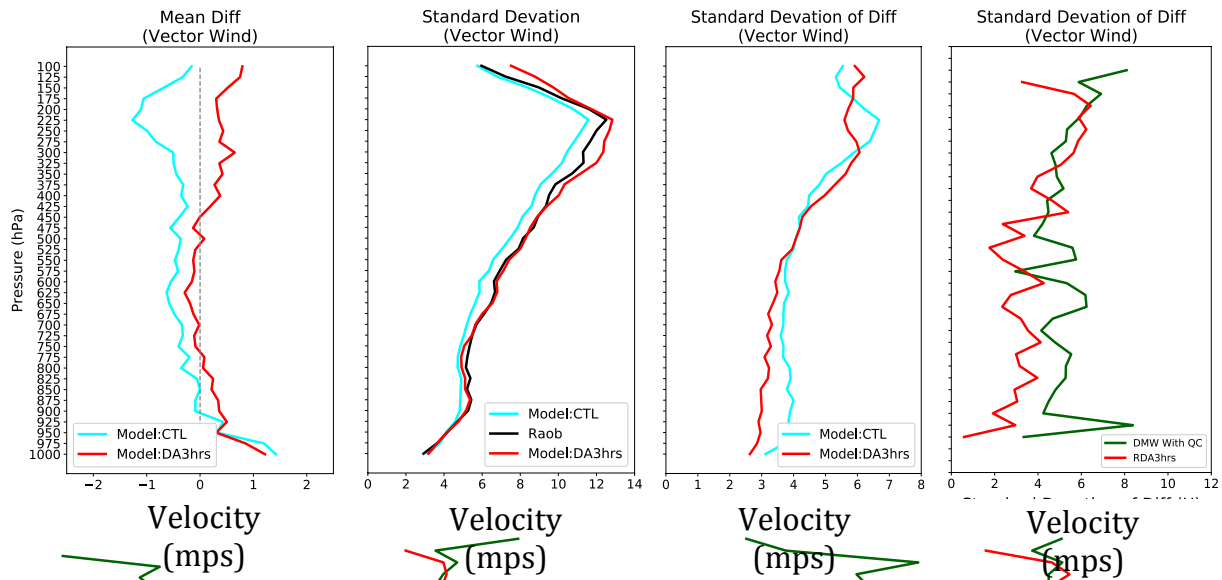


**Figure 2.** Comparison of differences between model diagnosed wind vectors and rawinsonde observations together with differences between cloud and water vapor feature tracked wind vector estimates and rawinsonde observations.

A typical example of the improvement of numerical forecasts through the three-hour continuous assimilation of high-resolution satellite sounding data is illustrated in figure 3 for 18 August 2020. These results were taken from the 8-km resolution WRF model run routinely at Hampton University on a 24/7 operational basis. It should be noted that these forecasts do not assimilate the PHSnABI temperature soundings (i.e., only the water vapor soundings are assimilated) for the reasons to be discussed in the next section of this paper. However, the PHSnABI water vapor soundings are given full weight (i.e., temperature and water vapor unbalance weights of 0 and 1.0, for PHSnABI temperature and humidity, respectively), for the modification of the forecast background humidity using the GSI assimilation system. Shown are the results of twelve forecasts for 12 UTC on August 18, each for lead times ranging between 1 and 12 hours. The forecasts conducted with the hourly assimilation of the high-resolution PHSnABI data are shown in the upper row of panels and compared with the operational RAP model forecasts for the same lead times as shown in the lower row of panels. It is important to note that the PHSnABI forecasts did not include any operational surface or upper air data (e.g., radiosonde and aircraft reports) after 21 UTC on August 17, which was the beginning of the 3-hour spin up period for the PHSnABI WRF forecasts, as shown in figure 1. Thus, the 00 UTC analysis used to initialize the 12-hour forecast for 12-UTC was based the RAP analysis at 21 UTC for the previous day and the 3-hour spin-up cycle of PHSnABI data assimilated at 21, 22, and 23 UTC. The inclusion of the RAP operational data prior to 22 UTC was implicit through the use of the RAP background analysis at 21 UTC for the assimilation of the PHSnABI data at 21 UTC, after which only the PHSnABI assimilated WRF forecasts was used as the background in the assimilation of the satellite data using GSI system. The improvement in the PHSnABI data assimilated WRF forecasts, relative to the operational RAP forecasts for 12 UTC can be seen most vividly in the forecast V-component of the of the wind, which is the variable most distinctly related to the forecast position and strength of storm systems. It is also obvious from figure 3 that there is

much more variance in the PHSnABI data assimilated forecasts for the 12 different initial times (i.e., 00 UTC to 11 UTC) which is expected because of the large amount of time independent sounding information going into the initialization of these forecasts relative to that going into the operational RAP forecasts, which do not assimilate the high-resolution and high-density PHSnABI sounding data.

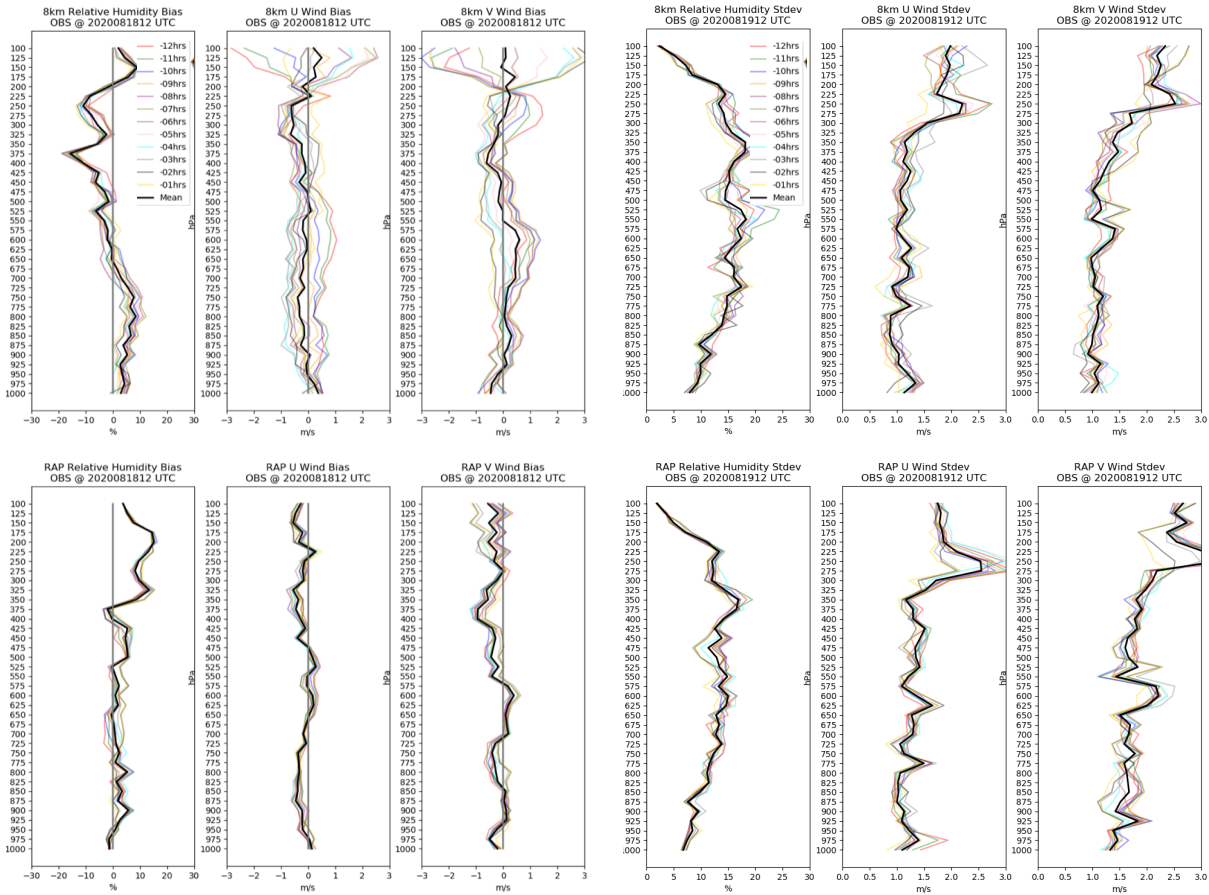


**Figure 3.** Twelve forecasts, ranging in lead-time from 12 hours to 1 hour, for 12 UTC August 18, 2020. The top row of panels illustrates the results of the PHSnABI sounding data assimilated WRF model forecasts whereas the lower row of panels illustrates the operational RAP forecast model results.

The characteristics of the PHSnABI sounding assimilated forecasts, relative to the RAP forecasts made without these high-resolution soundings, as shown in figure 3 for August 18, 2020, are typical. Figure 4 shows the comparisons of the mean 12 (1-hour to 12-hour lead-time) forecasts for 00 UTC and 12 UTC with the verification radiosonde observations for 5 consecutive days (18-22 August). Thus, the mean (bias) and standard deviation (Stdev) of forecast minus radiosonde differences for 120 different 12-hr forecast cycles are shown in figure 4. As stated earlier, the differences in the forecast initial states are due to the fact that the WRF forecasts (top row of panels) have the PHSnABI data assimilated hourly but do not assimilate the latest available radiosonde data, whereas the RAP forecasts do not have the benefit of the PHSnABI

sounding data but do benefit from the direct assimilation of the latest available 00 UTC and 12 UTC radiosonde observations to define their initial states. However, PHSnABI retrievals themselves benefit from the indirect use of radiosonde observations through the RAP operational 2-hr forecasts used to de-alias the polar satellite CrIS and IASI profile retrievals used in the PHSnABI fusion process.

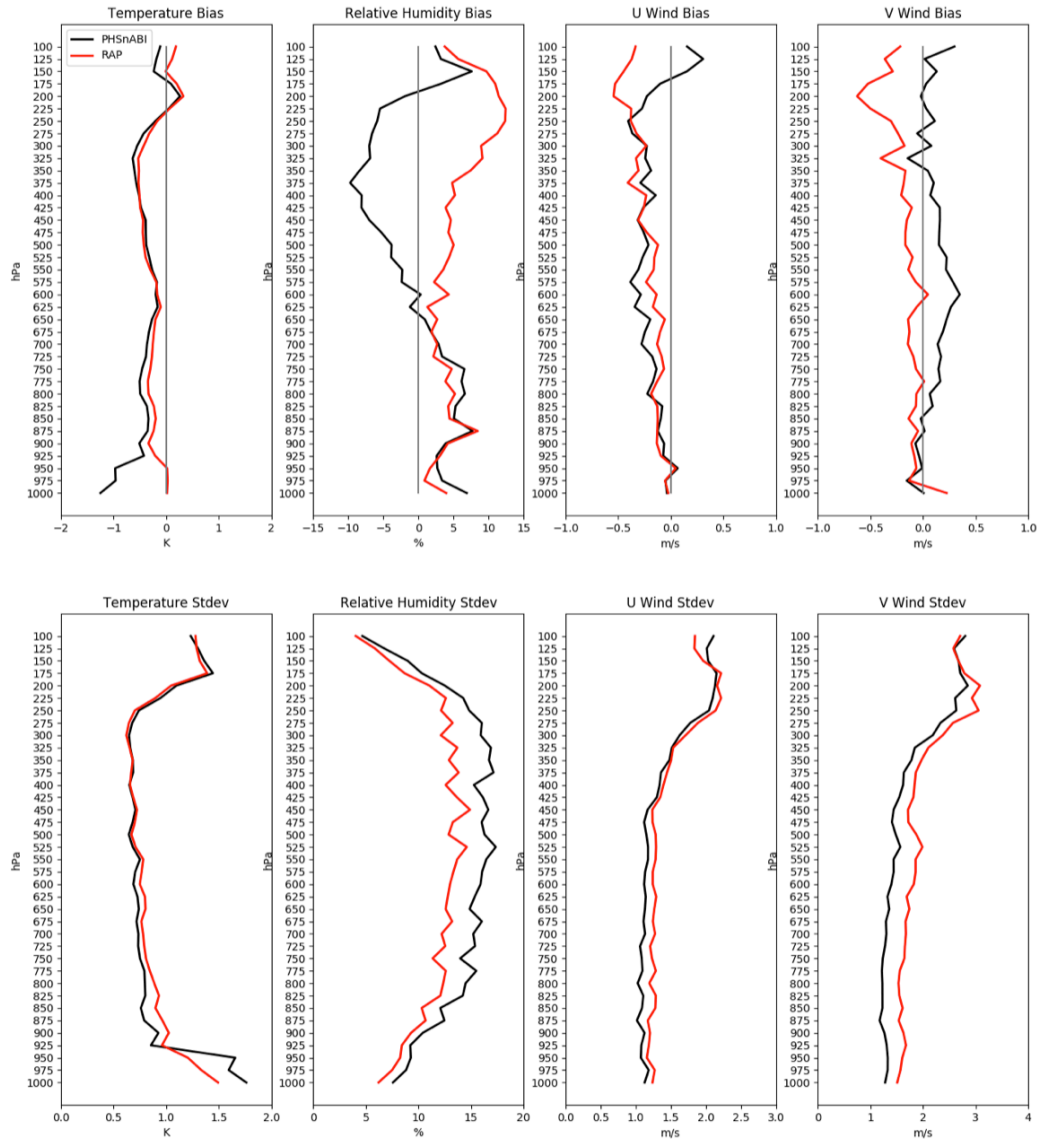


**Figure 4.** The mean (bias) and Standard Deviation (Stdev) of the differences between forecast temperature, relative humidity, and U and V wind components at 00 UTC and 12 UTC 00 UTC and 12 UTC radiosonde observations, for 120 different initialization times for 5 consecutive days (18-22 August).

As shown in figure 4, there are significant differences in the quality of the wind vector forecasts (the third and fourth panels) and these differences must be related to the difference in humidity forecasts (panel 2). Contrary to what might be expected, the standard deviation of the forecast differences with the radiosonde is larger for the RF than they are for the RAP. The bias difference between the RAP and WRF forecasts is believed to be related to the errors in

radiosonde humidity observations and the corrections applied during the RAP GSI assimilation process. It can be seen that the differences in these bias differences between the RAP and the WRF forecasts are small for the lower troposphere where the radiosonde humidity errors are known to be small. The fact that the standard deviation of the radiosonde difference of the WRF 8-km resolution humidity forecasts is larger than the RAP 13-km forecasts is believed to be due to the smaller horizontal features forecast by the WRF model, initialized by assimilating 2-km horizontal resolution satellite soundings. Since the horizontal space and time variance of the WRF humidity forecasts is larger than the that for the RAP forecasts, it is more likely to have larger differences with the radiosonde due to location and time discrepancies between the radiosonde observations and the forecast model grid point values. The fact that the standard deviation of the U and V component wind forecast errors, as validated using radiosonde observations, are significantly smaller than the standard deviation of the RAP forecast wind errors leads to the conclusion that the PHSnABI humidity is actually a more accurate representation of the true humidity state of the atmosphere than can be diagnosed without the use of the satellite sounding observations. The fact that mean (i.e., bias) errors of the RAP forecast wind components is slightly smaller than that for the PHSnSBI WRF forecasts, may be due to the direct use of the latest radiosonde observations in the RAP model initialization, which were not used for the WRF model initialization of the 12-hr forecast cycles being compared.

**Influence of GSI Temperature and Water Vapor Observation Weights on Convective Storm Forecasting:** The Grid point Statistical Interpolation (GSI) is a variational data assimilation system used in a variety of NWP systems, including NOAA's GFS, RAP, and HRRR forecast systems as well as the WRF model used here for the assimilation of satellite sounding retrievals. Incorporated in the GSI is a scheme that involves weighting the observations relative to the model background based on a background error covariance characterized by a balanced (i.e., large scale) and unbalanced (convective scale) partition, which can be adjusted using a partition weighting number that controls the relationships between the analysis control variables (i.e., stream function, temperature, water vapor, and surface pressure). The GSI default temperature and water vapor weighting for the adjustment of the temperature and water vapor weighting was set for temperature and humidity at 0.75 for the unbalanced portion of the covariance matrix used in the variational assimilation approach. A weight of zero for a particular input variable (e.g., temperature or humidity) means that the balanced partition will dominate the assimilation of that input variable. Experience over the past two years of assimilating the polar hyperspectral plus ABI fused satellite sounding profiles into the RAP-like WRF model showed that more skillful STP (i.e., Significant Tornado Parameter) and precipitation forecasts were obtained when only the water vapor retrievals were assimilated (i.e., by excluding the satellite temperature retrievals from the assimilation process). Although this result was not very satisfying from a physical expectation point of view (i.e., better forecasts were achieved by excluding, rather than including, the temperature retrievals) it was thought to result from the fact that the difference between the forecast temperature background and the PHSnABI temperatures being assimilated is already small. However, in conducting the SSEC2022 satellite sounding forecast impact analyses of the classic May, 20, 2013 Moore OK tornado outbreak, it was found that the convective weather forecast skill was highly dependent on the GSI control variable assimilation data weights assigned to the satellite temperature and water vapor retrievals.

Figure 3 shows the results of 3-hour forecasts of the convective weather associated with the Moore OK tornado outbreak, as illustrated through the forecast Radar reflectivity assuming different satellite temperature and moisture sounding data weights used in the GSI variable assimilation process. It can be seen all the forecasts regardless of the weights chosen, provide a forecast reflectivity at the tornado outbreak time which agrees better with the OKC radar (KTLX) image than does the control forecast (i.e., the forecast based on an initial condition which was devoid of the satellite sounding data). However, it can also be seen that the default 0.75 weighting of the unbalanced partition for temperature and water vapor humidity observations equally, also produced a very poor forecast of the Radar reflectivity whereas the forecast which excluded the temperature profiles (i.e., the Satellite water vapor - only panel) produced a relatively good forecast of the Radar reflectivity. One can see from figure 3 that the ability to forecast convective cells shown in the Radar image is quite dependent on the temperature and moisture weights used. The forecast Radar reflectivity most similar to the Radar reflectivity observation seems to be obtained when weights of 0.05 and 0.95 for the satellite temperature and humidity retrievals, respectively.

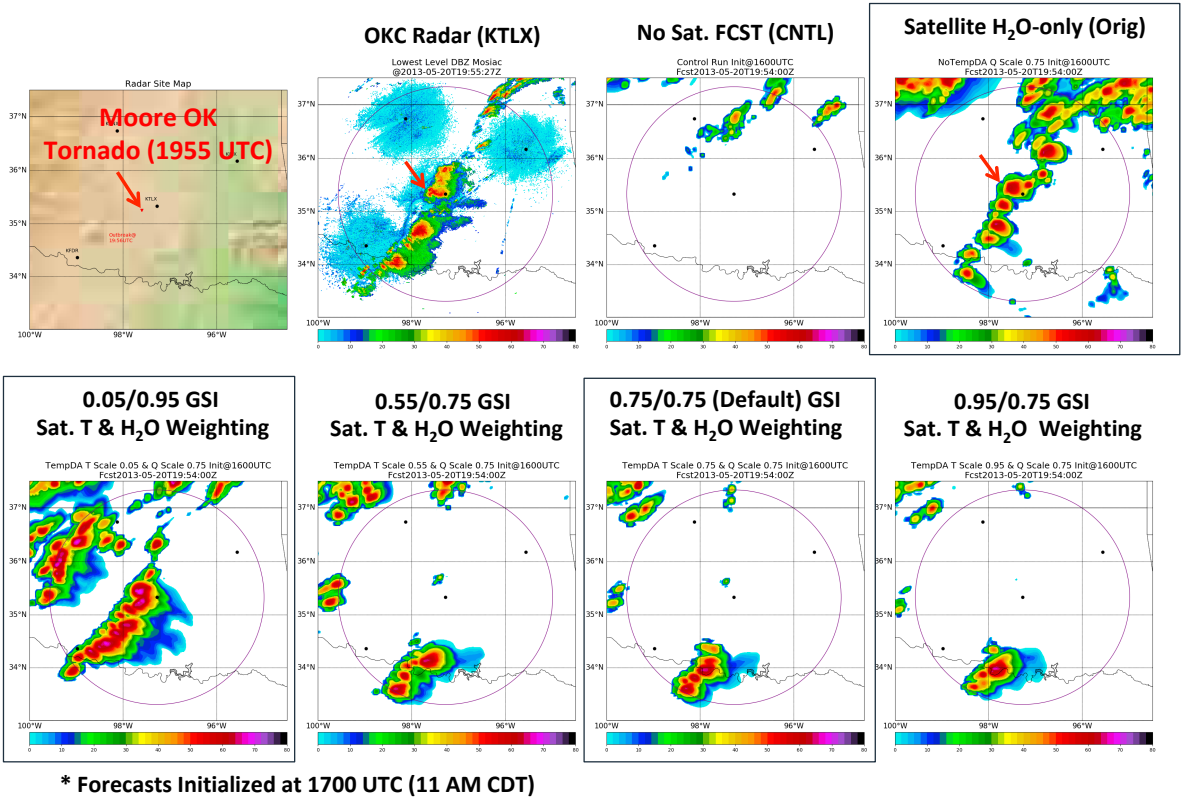


**Figure 3.** Observed and 3-hour forecast Radar reflectivity at the time of the Moore OK tornado which occurred at 1955 UTC (~ 2 PM) on May 20, 2013.

This same analysis was also applied to other Tornado cases, which occurred during 2020, including the March 3, 2020 Nashville Tornado and the Arkansas, Iowa, and northern Illinois March 28/29, 2020 tornado outbreak which resulted in showing the same dependence on the temperature and water vapor weighting of the unbalanced partition control variables as is shown here for the May 20, 2013 case.

## 2020 Tornado Outbreak Examples

Tornados are forecast using the Significant Tornado Parameter (STP), calculated from the forecast temperature, moisture, and wind fields, which indicate where severe convective cells spawning tornados will form. The first dramatic example of these STP forecasts obtained using high-resolution satellite sounding data in the real-time JPSS PGRR project's 8-km WRF forecast system was obtained on March 3, 2019, when a tornado outbreak, which killed 23 people, occurred across the SE USA. It was shown that the inclusion of high-resolution satellite sounding data produces a more accurate location of tornado development by reducing the false alarm area of high STP associated with the operational forecast (Smith. et. al., 2020). One year later (on March 3, 2020) another tornado occurred near Nashville TN killing 23 people. Figure 2 illustrates the STP forecasts obtained in real-time for this case, showing that the forecast that included the satellite sounding data pinpointed the highest STP to tornado location, as indicated by the NOAA Storm Prediction Center (SPC) (i.e., the red dot shown on this figure). For comparison, the RAP forecast, which did not benefit from the satellite sounding data, placed the highest STP to the west of the tornado location. Since the area of tornado development was quite cloudy for several hours prior to this development, the improved forecasts result from the soundings obtained prior to the time of the outbreak above clouds and down to the Earth's surface at some distance away from the tornado outbreak area. Because of the four dimensionality of the forecast model, more precise definition of the locations of convectively stable air using timely high spatial resolution soundings, act to better define the geographical limits of convectively unstable air, which improves the forecast location and time of STP maxima, where tornadoes are most likely. As shown in figure 2, the 2 to 6-hour forecasts indicated that the maximum STP would occur at Nashville TN at a time within in 1-hr of the actual time of the tornado development. In summary, both the location and time of the maximum STP associated with tornado occurrence should also be predicted with improved skill using the satellite sounding data in an operational forecast system, such as the NOAA RAP.

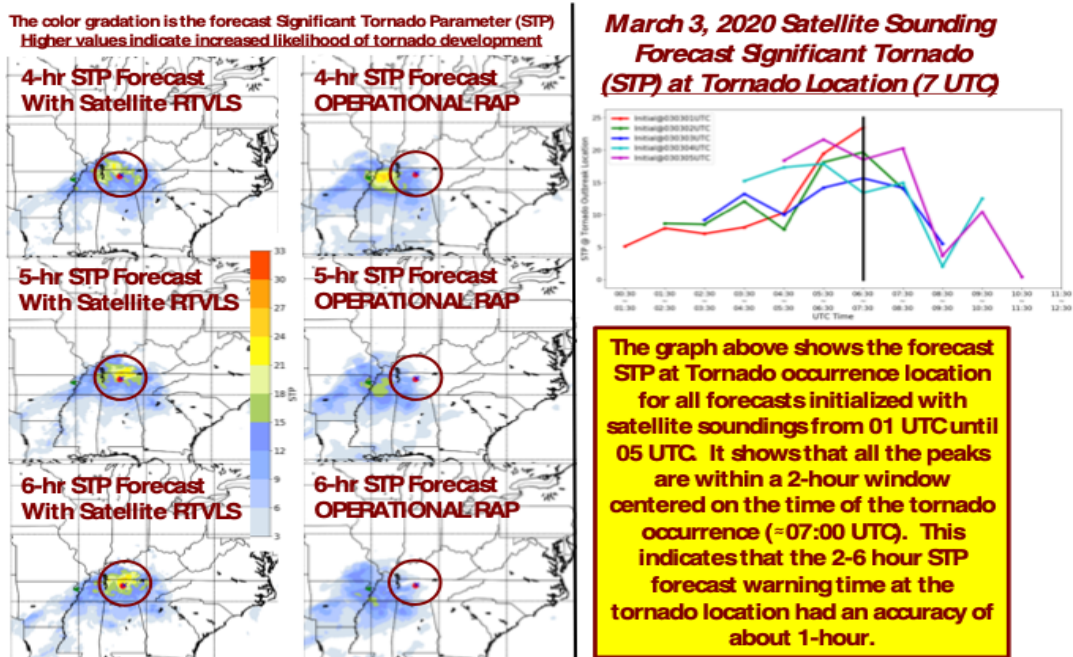


**Figure 4.** Real-time forecast of STP on March 3, 2020 using the HU/UW JPSS PGRR WRF.

Another tornado outbreak occurred On March 28, 2020. A large EF3 tornado struck the city of Jonesville AK. The same storm that produced this tornado also produced two EF1 tornadoes, one before and one after it moved over Jonesboro. Numerous tornadoes touched down in Iowa and Illinois, another in southwest WI. This included an EF1 tornado in Oelwein IA. An EF2 tornado touched down in Corydon KY, and another EF2 struck the town of Newburgh, IN, and an EF1 tornado also touched down in Peoria IL. The SPC severe weather reports and the WRF forecast STP, together with the operational RAP forecast STP, is shown in figure 5. It can be seen that the satellite sounding data assimilated WRF forecast high STP areas are in good correspondence to the ground-based observer severe weather reports.

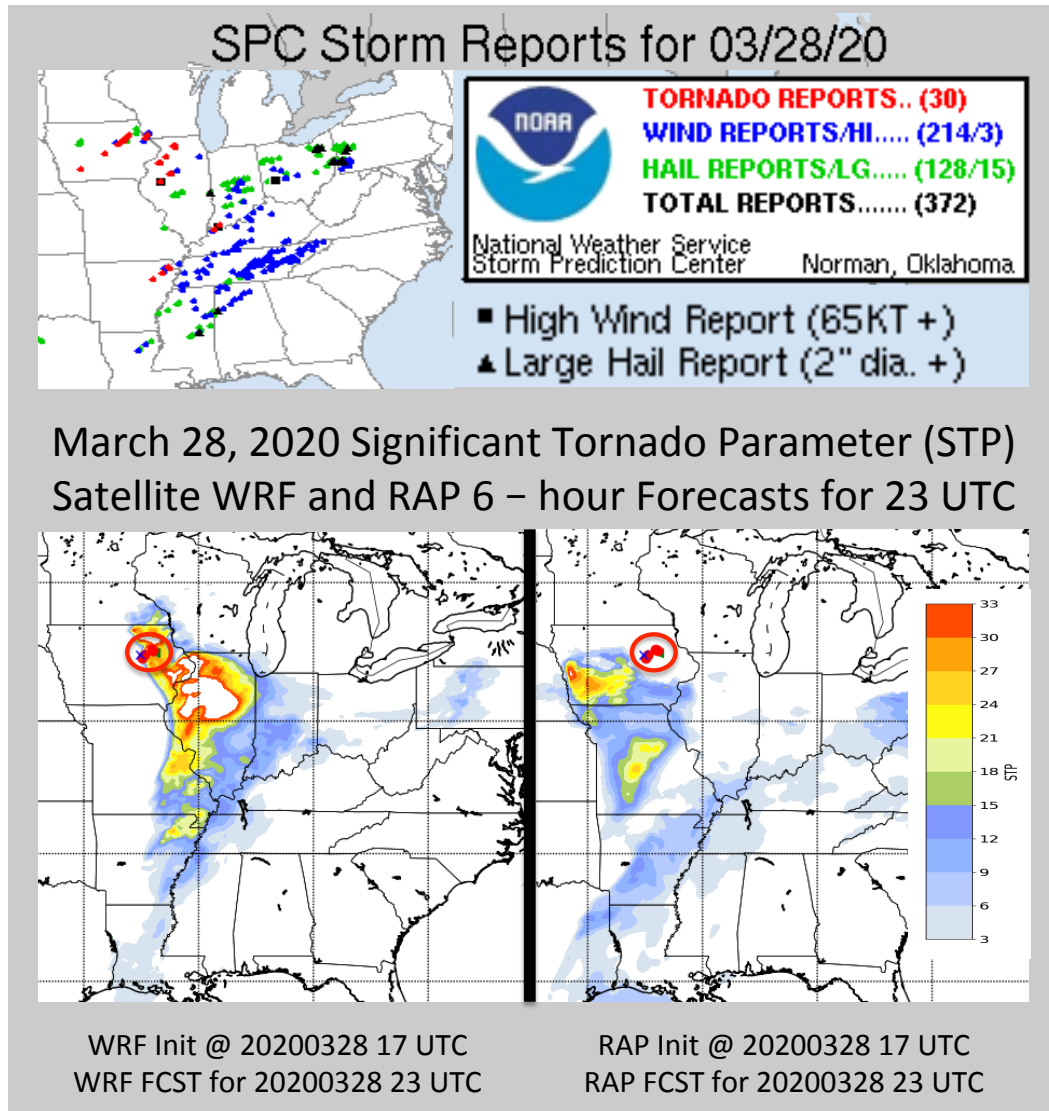


**Figure 5.** SPC severe weather reports and WRF and RAP forecast STP. Note that the white color saturated region in the high STP region in Illinois corresponds to STP values above 33.

The forecasts for March 3 and March 28 shown in figures 4 and 5 were re-run with a 3-km HRRR-configured WRF model in which the days PHSnABI data were assimilated to provide the initial conditions for each hourly interval forecast cycle. In this case the forecasts were compared with a control forecast produced from exactly the same WRF model used with the assimilated satellite soundings but without assimilating these data. The STP forecasts obtained with the 3-km forecast WRF model were similar to those obtained with the 8-km WRF model shown above. In order to illustrate the forecast improvement obtained by assimilating the forecast sounding data for the March 3 and March 28 Tornado outbreak days, figure 6 shows the verification of the U and V component wind forecasts for the two forecasts (i.e., ‘PHSnABI’ and the ‘Control’) at the radiosonde observation times closest to the tornado outbreaks for each day (i.e., 12 UTC and 000 UTC, respectively). Radiosonde reports were used to produce these statistics. One can see that the biggest improvement shown by the ‘PHSnABI’ sounding assimilated forecasts over the

‘control’ is for the ‘V’ component of the wind, which is most highly related to the strength and position of the convective storm systems producing these tornado outbreaks on each day.

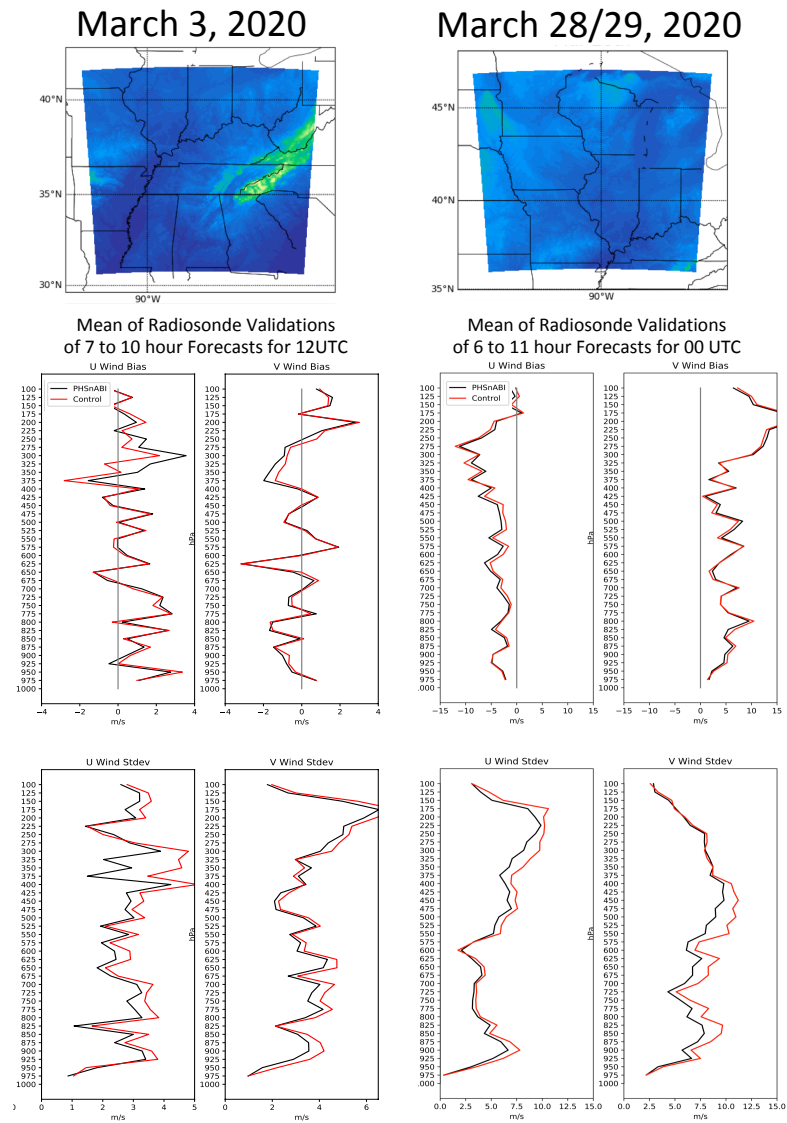


**Figure 6.** Mean (Bias) and Standard Deviation of the difference between U and V components forecast winds compared to radiosonde observations for each day.

## Summary and Conclusion

It has been shown through that forecasts of real-time Direct Broadcast Satellite (DBS) sounding data RAP-configured and HRRR-configured WRF model forecasts that significant improvements in convective weather forecasts are obtained through the assimilation for these data. These improvements have been validated using both SPC surface severe weather reports and radiosonde wind observations.

Because these improvements in forecasts have been demonstrated continuously on a real-time routine basis for a two-year period, it is time to enter a RTO test phase of this NOAA JPSS

PGRR project. During the RTO phase, both the production of the high-resolution satellite soundings and their assimilation into NOAA operational models need to be demonstrated jointly by NOAA NESDIS and NOAA NCEP. It is proposed to conduct this RTO demonstration of operational readiness during the next three-year period of the NOAA JPSS PGRR program.

## References:

Benjamin, S. G., and Coauthors, 2016: A North American Hourly Assimilation and Model Forecast Cycle: The Rapid Refresh. *Mon. Wea. Rev.*, **144**, 1669–1694, <https://doi.org/10.1175/MWR-D-15-0242.1>.

Geer, A.J., K. Lonitz, P. Weston, M. Kazumori, K. Okamoto, Y. Zhu, E.H. Liu, A. Collard, W. Bell, S. Migliorini, P. Chambon, N. Fourri, M.-J. Kim, C. Köpken-Watts & C. Schraff, 2018: All-sky satellite data assimilation at operational weather forecasting centres. *Q.J.R. Meteorol. Soc.*, **144**, 1191–1217, doi:10.1002/qj.3202.

James, E. P., and S. G. Benjamin, 2017: Observation System Experiments with the Hourly Updating Rapid Refresh Model Using GSI Hybrid Ensemble–Variational Data Assimilation. *Mon. Wea. Rev.*, **145**, 2897–2918, <https://doi.org/10.1175/MWR-D-16-0398.1>.

Le Marshall, J., and Coauthors, 2007: THE JOINT CENTER FOR SATELLITE DATA ASSIMILATION. *Bull. Amer. Meteor. Soc.*, **88**, 329–340, <https://doi.org/10.1175/BAMS-88-3-329>.

Lin, H., S. S. Weygandt, S. G. Benjamin, and M. Hu, 2017: Satellite Radiance Data Assimilation within the Hourly Updated Rapid Refresh. *Wea. Forecasting*, **32**, 1273–1287, <https://doi.org/10.1175/WAF-D-16-0215.1>.

Migliorini, S., 2011: On the equivalence between radiance and retrieval assimilation. *Monthly Weather Review*, **140**, 258–265.

Rodgers, C. D., Characterization and error analysis of profiles retrieved from remote sounding measurements, *J. Geophys. Res.*, **95**, 5587–5595, 1990.

Rodgers, C. D. 2000: Inverse Methods for Atmospheric Sounding - Theory and Practice, World Scientific Press, 2000.

Rodgers, C. D. and B. J. Connor, 2003: Intercomparison of remote sounding instruments, *J. Geophys. Res.*, **108**, D3, 4116, doi:10.1029/2002JD002299

Smith, W. L., E. Weisz, S. V. Kireev, D. K. Zhou, Z. Li, and E. E. Borbas, 2012: Dual-Regression Retrieval Algorithm for Real-Time Processing of Satellite Ultraspectral Radiances. *J. Appl. Meteor. Climatol.*, **51**, 1455–1476, <https://doi.org/10.1175/JAMC-D-11-0173.1>.

Smith, W. L., E. Weisz, and H. Revercomb, 2015: The retrieval of atmospheric profiles from

satellite radiances for NWP data assimilation. *Proc. 20th Int. TOVS Study Conf.*, Lake Geneva, WI, International TOVS Working Group, 4.04.

Smith, W. L., and E. Weisz, 2017: Dual Regression Approach for High Spatial Resolution Infrared Soundings, in *Comprehensive Remote Sensing*, M. Goldberg, Editor, Elsevier Ltd, Langford Lane Oxford, OX5 1GB UK.

Smith, W. L., Q. Zhang, M. Shao, and E. Weisz, 2020: Improved Severe Weather Forecasts Using LEO and GEO Satellite Soundings. *J. Atmos. Oceanic Technol.*, **37**, 1203–1218, <https://doi.org/10.1175/JTECH-D-19-0158.1>.